Journal of Sound and Vibration 329 (2010) 5225–5232

Contents lists available at ScienceDirect

Journal of Sound and Vibration

journal homepage: www.elsevier.com/locate/jsvi

Rapid Communication

On the functional form of a nonlinear vibration absorber

R. Viguié *, G. Kerschen

Space Structures and Systems Laboratory, Structural Dynamics Research Group, Aerospace and Mechanical Engineering Department, University of Liège, Liège, Belgium

ARTICLE INFO

Article history:
Received 16 February 2010
Received in revised form
6 July 2010
Accepted 6 July 2010
Handling Editor: L.N. Virgin
Available online 24 July 2010

ABSTRACT

Due to the frequency–energy dependence of nonlinear oscillations, nonlinear dynamical absorbers present interesting properties for mitigating unwanted vibrations in mechanical systems. Unlike the tuned mass damper, the functional form of a nonlinear absorber is not known a priori and must be determined. This short note addresses this issue when a light-weight nonlinear absorber is attached to a nonlinear primary structure. Numerical simulations demonstrate that the determination of an adequate functional form may be directly linked to the frequency–energy dependence of the primary structure.

1. Introduction

Realizing the limitations of the tuned mass damper (TMD) [1,2], nonlinear vibration absorbers have been developed for their ability to enlarge the suppression bandwidth. The first studies date back to Roberson [3], Pipes [4] and Arnold [5]. Since then, nonlinear absorbers have received increasing attention in the literature (see, e.g., the autoparametric vibration absorber [6–8] and the nonlinear energy sink [9–12]). One potential limitation of nonlinear vibration absorbers is that their performance depends critically on the total energy present in the system or, equivalently, on the amplitude of the external forcing. This stems from the frequency–energy dependence of nonlinear oscillations, which is one typical feature of nonlinear dynamical systems.

Because the functional form of a nonlinear absorber is not known a priori, its determination is an important issue. Although other functional forms were examined in the literature, a cubic stiffness is often chosen for the realization of a nonlinear absorber [13]. In this context, Viguié et al. [14] showed that, through an adequate selection of the functional form, a nonlinear absorber can mitigate the vibrations of a specific mode of a nonlinear primary structure in a wide range of excitation amplitudes. A frequency–energy-based tuning methodology was proposed, such that the nonlinear absorber possesses the same frequency–energy dependence as that of the considered mode of the primary structure. The objective of this short note is to further investigate the effectiveness of the proposed methodology using detailed numerical simulations. Specifically, we propose to compare the performance of dynamical absorbers presenting different functional forms.

The paper is organized as follows. In Section 2, the performance of three absorbers, namely a TMD, an absorber with hardening nonlinearity and an absorber with softening nonlinearity, is compared when these devices are coupled to a primary structure possessing hardening nonlinearity. Once an appropriate functional form is determined, the optimal value of the nonlinear coefficient is sought, which is carried out in Section 3. To further validate the proposed methodology, a primary structure possessing softening nonlinearity is considered in Section 4. The conclusions of the present study are summarized in Section 5.

* Corresponding author. Tel.: +32 4 3664854; fax: +32 4 3664856.
E-mail addresses: r.viguie@ulg.ac.be (R. Viguié), g.kerschen@ulg.ac.be (G. Kerschen).

0022-460X/$ - see front matter © 2010 Elsevier Ltd. All rights reserved.
doi:10.1016/j.jsv.2010.07.004

2. Determination of the functional form of the dynamical absorber

The system considered herein is composed of a nonlinear single-degree-of-freedom (SDOF) system, which is coupled to three absorbers, namely a TMD, an absorber with hardening nonlinearity and an absorber with softening nonlinearity (see Figs. 1(a)–(c), respectively). Without lack of generality, the primary system is chosen to be essentially nonlinear

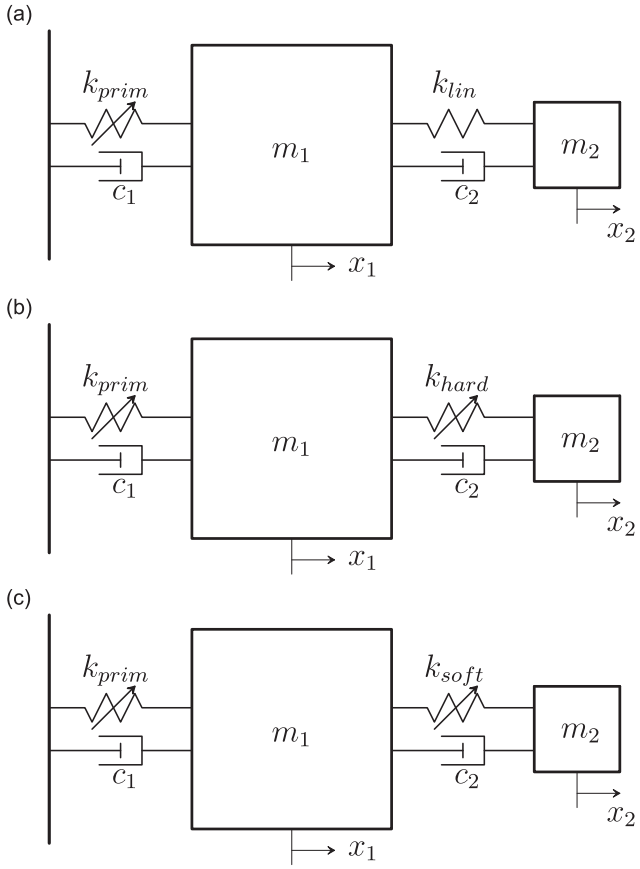

Fig. 1. Essentially nonlinear oscillator coupled to (a) a tuned mass damper; (b) a nonlinear hardening absorber and (c) a nonlinear softening absorber.

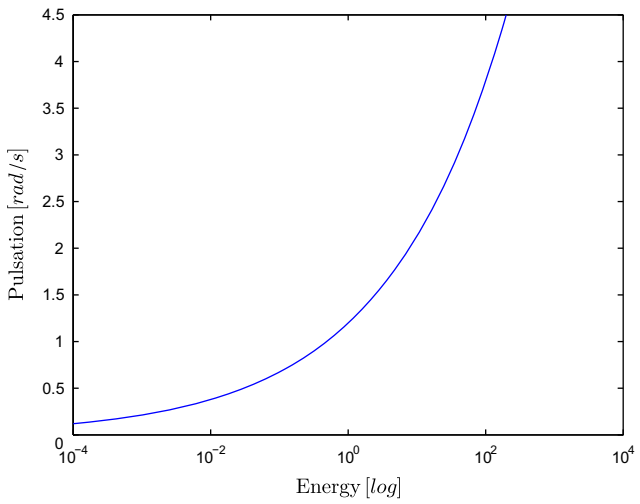

Fig. 2. Backbone curve of the nonlinear primary structure.

(i.e., the restoring force is realized using a cubic stiffness); its backbone curve is represented in the frequency–energy plot (FEP) of Fig. 2. A light-weight absorber is considered for obvious practical reasons, and slight damping is introduced to induce energy dissipation. The system parameters are listed in Table 1. The system is subjected to an impulsive load modeled as a nonzero initial condition on the velocity of the primary system $\dot{x}_1(0) \neq 0, x_1(0) = x_2(0) = \dot{x}_2(0) = 0$.

The objective consists in determining which absorber leads to effective vibration mitigation for various energy levels. The performance and robustness of a specific absorber are assessed in this study through three-dimensional plots representing the energy dissipated in the absorber against two parameters, namely the nonlinear stiffness of the primary system and the impulse amplitude. The latter parameter is in direct relation with the energy injected in the structure, whereas the former parameter is representative of a potential mistuning (due to, for instance, the ageing of the structure).

Table 1
System parameters.

Parameter	Units	Value
m_1	(kg)	1
k_{prim}	(N/m^3)	1
c_1	(Ns/m)	0.002
m_2	(kg)	0.05
c_2	(Ns/m)	0.002

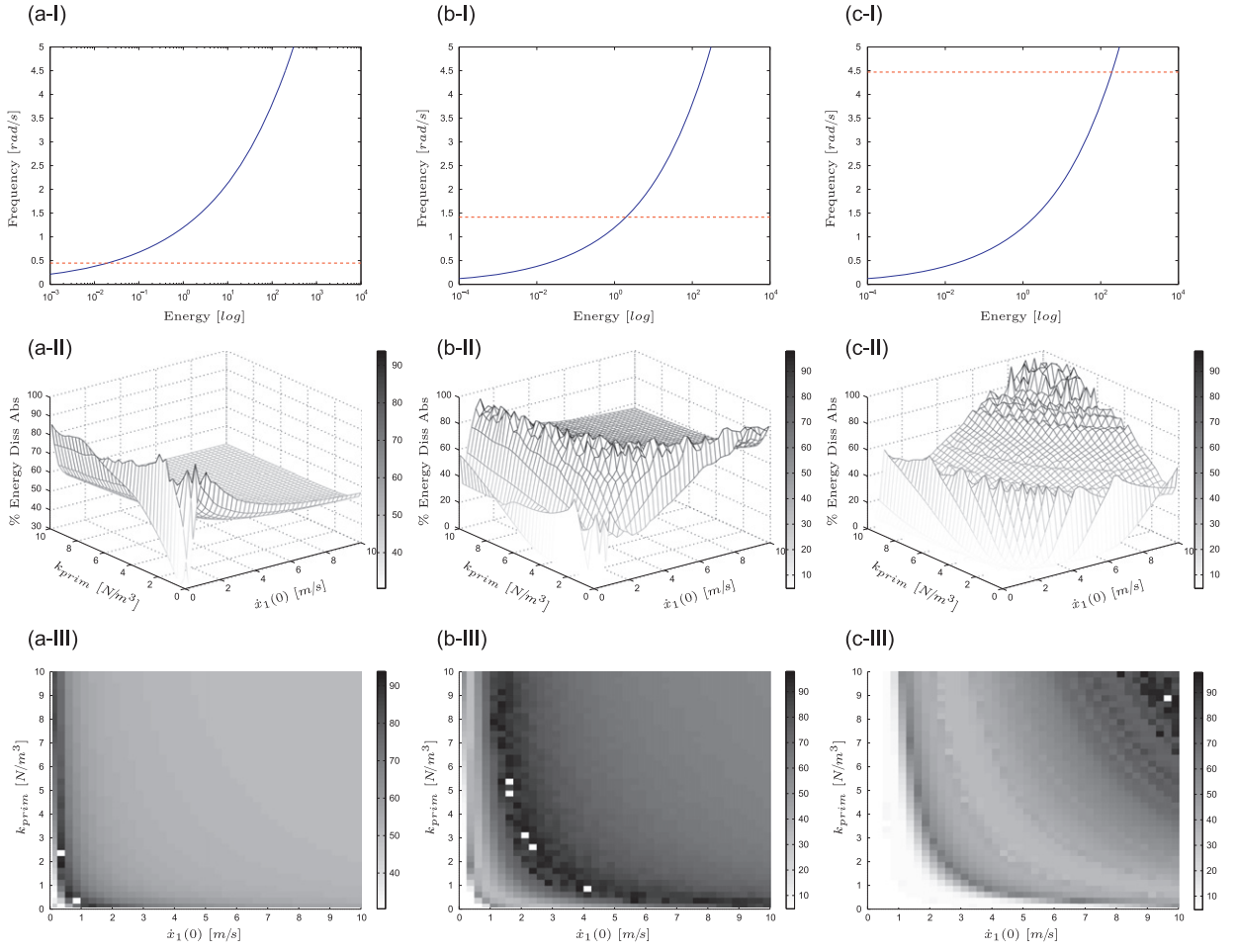

Fig. 3. Energy dissipation in a TMD coupled to a nonlinear oscillator. (a) k_{lin}=0.01 N/m, (b) k_{lin}=0.1 N/m and (c) k_{lin}=1 N/m. Subfigures (I) depict the backbone curve of the nonlinear oscillator (blue solid line) and the TMD (red dashed line). Subfigures (II) illustrate the percentage of energy dissipated in the absorber against the nonlinear stiffness of the primary structure k_{prim} and the impulse magnitude $\dot{x}_1(0)$. Subfigures (III) represent two-dimensional projections of subfigures (II). (For interpretation of the references to colour in this figure legend, the reader is referred to the web version of this article.)

2.1. Performance of the tuned mass damper

A TMD is first coupled to the primary structure. It seems that no formal procedure exists in the literature for the design of a TMD coupled to a nonlinear oscillator. In this context, a parametric approach is adopted by considering three different (linear) stiffnesses for the TMD. The dynamics of the resulting system is shown in Fig. 3. Subfigures (I) clearly show the frequency mismatch: the frequency of the primary structure increases with energy due to the hardening nonlinearity, whereas the TMD does not exhibit any frequency–energy dependence. This frequency mismatch is also evident in Subfigures (II) and (III) through the variability of the energy dissipated in the TMD with the impulse magnitude.

In addition, Fig. 3 highlights that there is a correspondence between the localization of the region where the two backbones intersect in Subfigures (I) and the localization of the region of high energy dissipation in Subfigures (II) and (III). Even though a quantitative analysis is not available so far, a qualitative analysis can be performed (using Figs. 4(a–c)) to explain this feature. Fig. 4(a) depicts the two intersecting points occurring between the frequency–energy dependence of the TMD (dashed black line) and the one of the nonlinear oscillator with two different nonlinear stiffness values (k_{prim}=1 (N/m^3) in solid red line and k_{prim}=10 (N/m^3) in dashed-dotted blue line). The direct neighborhood of the intersecting points (resonant points) is highlighted by black dotted circles. In these regions, both oscillators may engage in resonance enabling strong interactions through beating phenomena, which results in high energy dissipation in the absorber. The intersecting points are located at specific energy levels (α and β) that can be directly related to the initial impulse magnitude $\dot{x}_1(0)$ through the kinetic energy (that equals the total energy in the system at t=0). At this stage, it

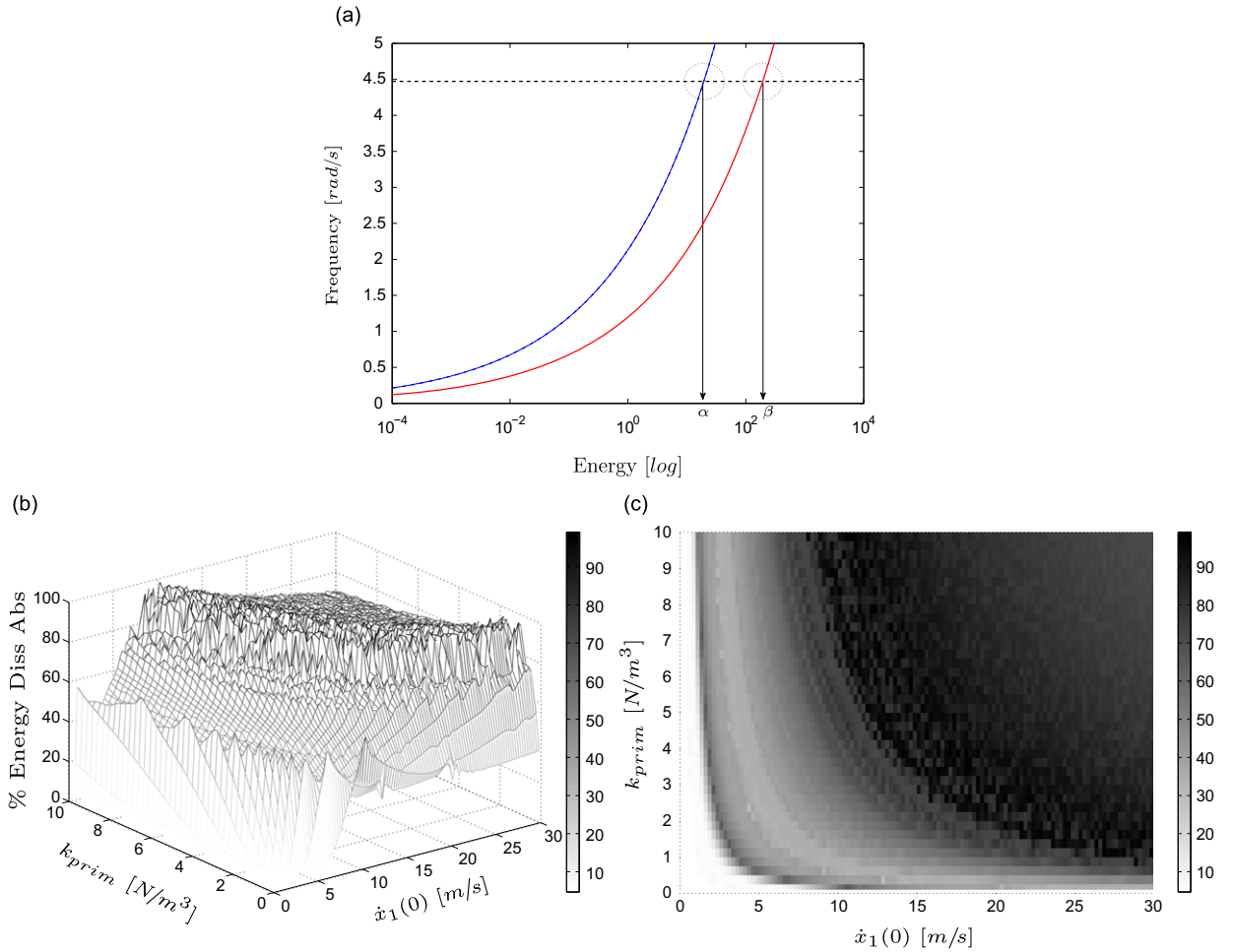

Fig. 4. Subfigure (a) depicts the backbone curve of the nonlinear oscillator (k_{prim}=10 (N/m^3): blue dashed-dotted line/k_{prim}=1 (N/m^3): red solid line) and the TMD (black dashed line). The black dotted circles show supposed zones of influence where strong interactions between the NL oscillator and the TMD occur. Subfigure (b) illustrates the percentage of energy dissipated in the absorber against the nonlinear stiffness of the primary structure k_{prim} and the impulse magnitude $\dot{x}_1(0)$. Subfigure (c) represents two-dimensional projections of subfigure (b). (For interpretation of the references to colour in this figure legend, the reader is referred to the web version of this article.)

appears that: (i) a high energy dissipation level occurs at specific couples $(\dot{x}_1(0), k_{\text{prim}})$ and (ii) because $\alpha < \beta$, the high energy dissipation level occurs at a lower impulse magnitude $(\dot{x}_1(0))$ for $k_{\text{prim}}=10\,(\text{N/m}^3)$ than for $k_{\text{prim}}=1\,(\text{N/m}^3)$. Subfigure 4(c) depicts this last feature. A high energy dissipation region is localized around $\dot{x}_1(0)=9\,(\text{m/s})$ for $k_{\text{prim}}=10\,(\text{N/m}^3)$, whereas it is located around $\dot{x}_1(0)=30\,(\text{m/s})$ for $k_{\text{prim}}=1\,(\text{N/m}^3)$.

As a concluding remark, the variation of the nonlinear stiffness k_{prim} induces changes in the backbone curve of the primary system and, consequently, in the localization of the resonance region. This gives rise in Subfigures (II) and (III) to a locus of points $(k_{\text{prim}}, \dot{x}_1(0))$ for which high energy dissipation occurs.

2.2. Performance of the absorber with softening nonlinearity

An absorber with softening nonlinearity is now attached to the nonlinear SDOF system. The functional form obeys a cubic root law, and three different numerical values $k_{soft}=0.01$, 0.1 and $1\,(\text{N/m}^{1/3})$ are considered. The results are presented in Fig. 5. These results are qualitatively similar to those of the previous section, and the same conclusions can be drawn. Specifically, the frequency mismatch is also observed for this softening absorber, which results in energy-dependent performance.

2.3. Performance of the absorber with hardening nonlinearity

The performance of the TMD and of the nonlinear softening absorber depends critically on the total energy present in the system. This section investigates if an absorber possessing a backbone curve similar to that of the primary system can resolve this limitation. Two different exponents (i.e., 3 and 7) for the nonlinearity are examined, and the results are

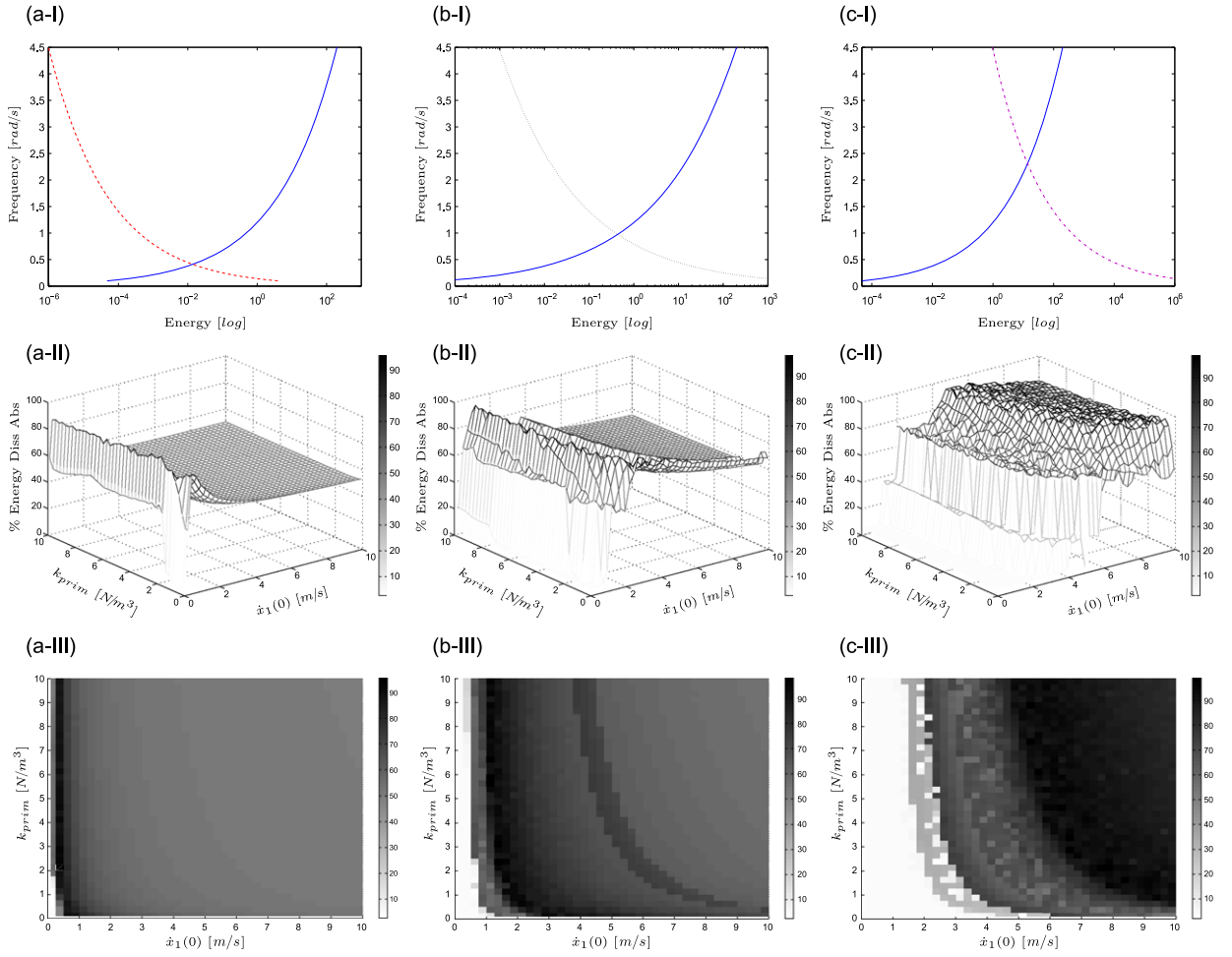

Fig. 5. Energy dissipation in an absorber with softening nonlinearity coupled to a nonlinear oscillator. (a) $k_{soft}=0.01\,\text{N/m}^{1/3}$, (b) $k_{soft}=0.1\,\text{N/m}^{1/3}$ and (c) $k_{soft}=1\,\text{N/m}^{1/3}$. Subfigures (I) depict the backbone curve of the nonlinear oscillator (blue solid line) and of the softening absorbers: red dashed line for $k_{soft}=0.01\,\text{N/m}^{1/3}$, black dotted line for $k_{soft}=0.1\,\text{N/m}^{1/3}$, violet alternated line for $k_{soft}=1\,\text{N/m}^{1/3}$. Subfigures (II) illustrate the percentage of energy dissipated in the absorber against the nonlinear stiffness of the primary structure k_{prim} and the impulse magnitude $\dot{x}_1(0)$. Subfigures (III) represent two-dimensional projections of subfigures (II). (For interpretation of the references to colour in this figure legend, the reader is referred to the web version of this article.)

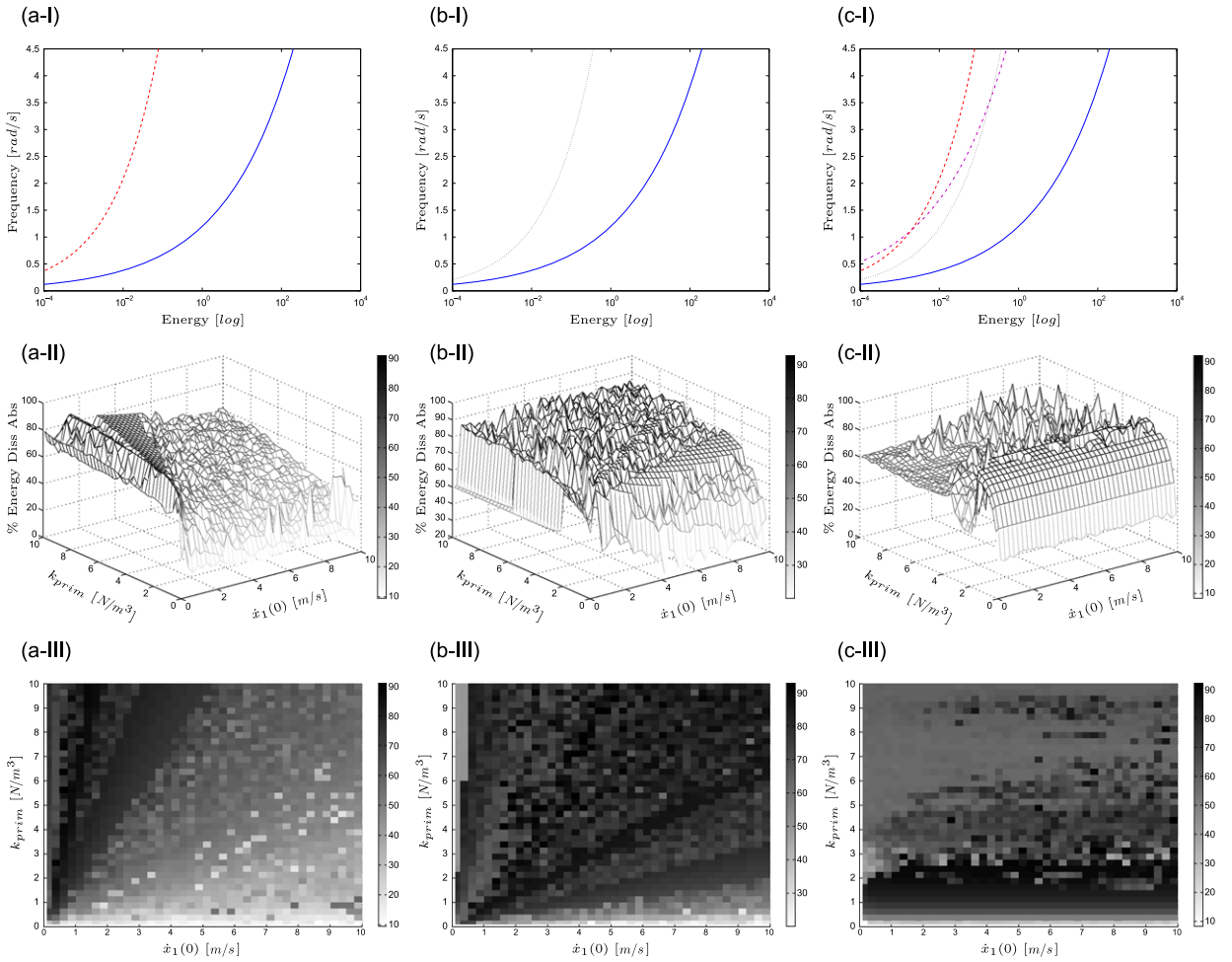

Fig. 6. Energy dissipation in an absorber with hardening nonlinearity coupled to a nonlinear oscillator. Subfigures (a) and (b) correspond to a nonlinear stiffness characterized by an exponent 7 with k_{hard} equal to 100 N/m^7 and 1 N/m^7, respectively. Subfigures (c) correspond to a cubic stiffness with k_{hard}=1 N/m^3. Subfigures (I) depict the backbone curve of the nonlinear oscillator (blue solid line) and of the hardening absorbers: red dashed line for k_{hard}=100 N/m^7, black dotted line for k_{hard}=1 N/m^7, violet alternated line for k_{hard}=1 N/m^3. Subfigures (II) illustrate the percentage of energy dissipated in the absorber against the nonlinear stiffness of the primary structure k_{prim} and the impulse magnitude $\dot{x}_1(0)$. Subfigures (III) represent two-dimensional projections of subfigures (II). (For interpretation of the references to colour in this figure legend, the reader is referred to the web version of this article.)

depicted in Fig. 6. Subfigures (a) and (b) correspond to an exponent equal to 7 with k_{hard} equal to 100 and 1 N/m^7, respectively. Even though the backbone curves of these absorbers do not match that of the primary system, the hardening behavior seems to induce positive effects. In Subfigures (a-(II–III)), a rather smooth and well-defined zone of high energy dissipation is identified. This zone is retrieved in Subfigures (b-(II–III)) at lower values of k_{prim} and spreads over a wider range of excitation levels. Subfigures (c) display the results obtained with a cubic absorber possessing the same functional form as that of the primary system. Clearly, there exists a smooth region where high energy dissipation occurs for all impulse magnitudes, which makes this absorber amplitude robust. This result is interesting, because it validates the qualitative tuning methodology proposed in [14].

3. Determination of the nonlinear coefficient k_{cub}

The previous section has highlighted that the functional form of the absorber is to be chosen according to the frequency–energy dependence of the primary structure. The nonlinear coefficient of the absorber is still to be determined to maximize both performance and robustness. Figs. 7(a)–(c) depict the results for three different nonlinear coefficients k_{cub}. It confirms that all three absorbers are effective; i.e., they can dissipate a large amount of the input energy for a certain range of values of the nonlinear coefficient k_{prim}. For decreasing values of k_{cub}, a contraction and a translation of the high energy dissipation region is observed.

Because the nominal value of the coefficient of the primary system is k_{prim}=1 (N/m^3) (see Table 1), it seems that an adequate value for the cubic stiffness is k_{cub}=0.01 (N/m^3). Although they are not in complete correspondence, Fig. 7(c-I) displays that the

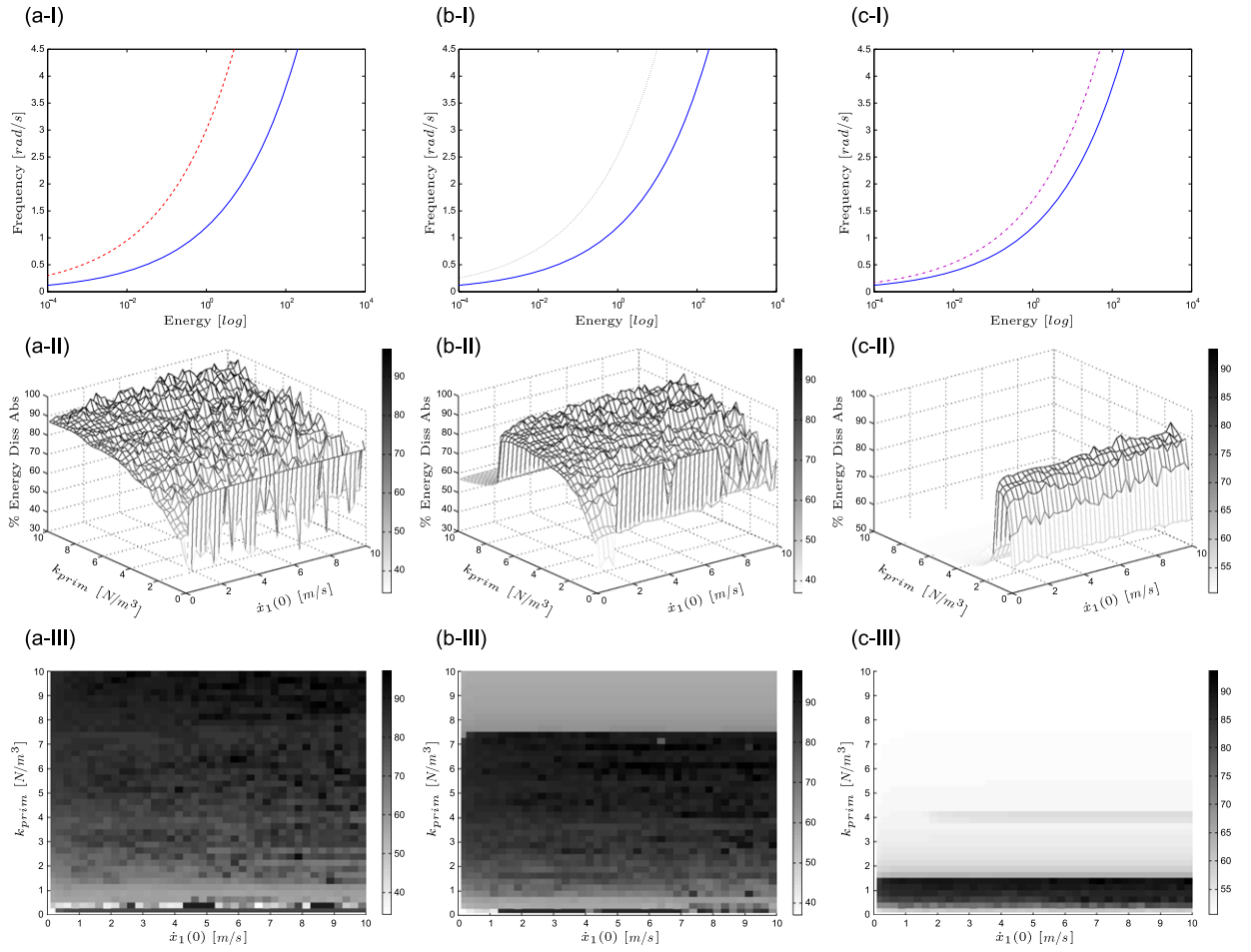

Fig. 7. Energy dissipation in an absorber with cubic nonlinearity coupled to a nonlinear oscillator. (a) k_{cub}=0.1 N/m^3, (b) k_{cub}=0.05 N/m^3 and (c) k_{cub}=0.01 N/m^3. Subfigures (I) depict the backbone curve of the nonlinear oscillator (blue solid line) and of the absorbers: red dashed line for k_{cub}=0.1 N/m^3, black dotted line for k_{cub}=0.05 N/m^3, violet alternated line for k_{cub}=0.01 N/m^3. Subfigures (II) illustrate the percentage of energy dissipated in the absorber against the nonlinear stiffness of the primary structure k_{prim} and the impulse magnitude $\dot{x}_1(0)$. Subfigures (III) represent two-dimensional projections of subfigures (II). (For interpretation of the references to colour in this figure legend, the reader is referred to the web version of this article.)

Table 2
System parameters.

Parameter	Units	Value
m_1	(kg)	1
k_{prim}	(N/m$^{1/3}$)	1
c_1	(Ns/m)	0.002
m_2	(kg)	0.05
k_{soft}	(N/m$^{1/3}$)	0.105
c_2	(Ns/m)	0.002

backbone curves of the two oscillators exhibit a similar frequency–energy dependence. More than 90% of the energy initially imparted in the primary oscillator is dissipated in the nonlinear absorber, and a remarkable result is that the performance does not depend on impulse magnitude. We note that these numerical results are in complete agreement with the analytical developments of Ref. [14].

4. Validation of the results for a primary oscillator with softening nonlinearity

A primary oscillator with softening nonlinearity (cubic root) is now examined. According to the previous developments, the nonlinear absorber should also present a nonlinearity with a cubic root. The system parameters are listed in Table 2.

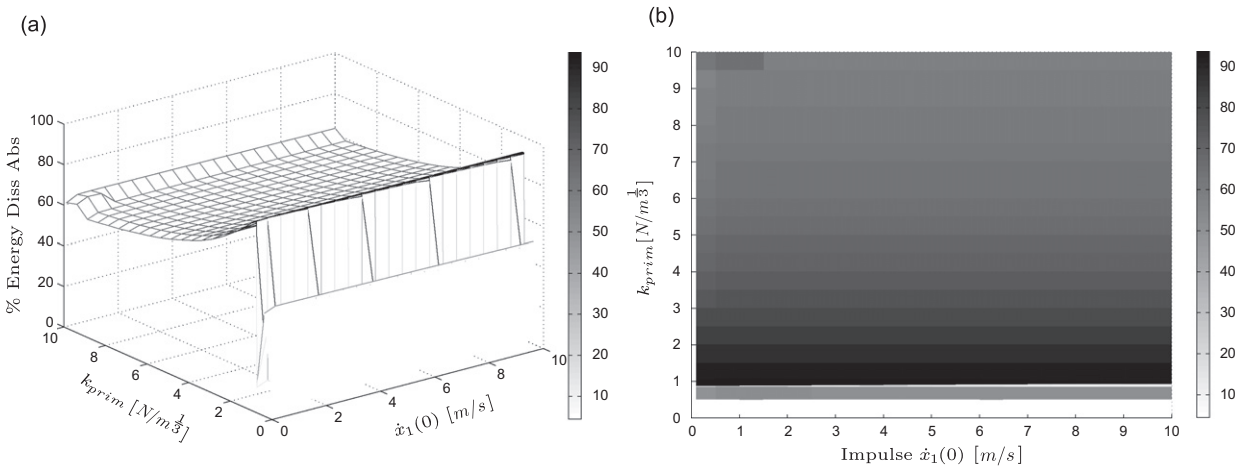

Fig. 8. Energy dissipation in an absorber with softening nonlinearity coupled to a nonlinear softening oscillator. (a) Percentage of energy dissipated in the absorber against the nonlinear stiffness of the primary structure k_{prim} and the impulse magnitude $\dot{x}_1(0)$; (b) two-dimensional projection.

Figs. 8(a–b) show that high energy dissipation is realized around $k_{\text{prim}} = 1\,(\text{N/m}^{1/3})$ and that the performance does not depend on the impulse magnitude.

5. Conclusion

This short note addressed the determination of an appropriate functional form of a nonlinear dynamical absorber when it is coupled to a nonlinear primary structure. The main finding is that the backbone curves of the primary system and of the absorber should exhibit a similar, though not identical, frequency–energy dependence. As a result, the absorber is capable of effectively mitigating the unwanted vibrations of the primary system in a wide range of excitation amplitudes.

Acknowledgment

The author R. Viguié would like to acknowledge the Belgian National Fund for Scientific Research (FRIA fellowship) for its financial support.

References

[1] H. Frahm, A Device for Damping Vibrations of Bodies, US Patent 989958, 1911.
[2] J.P. Den Hartog, *Mechanical Vibrations*, fourth ed., Dover Books on Engineering, 1985.
[3] R. Roberson, Synthesis of a nonlinear dynamic vibration absorber, *Journal of the Franklin Institute* 254 (1952) 205–220.
[4] L. Pipes, Analysis of a nonlinear dynamic vibration absorber, *Journal of Applied Mechanics* 20 (1953) 515–518.
[5] F. Arnold, Steady-state behavior of systems provided with nonlinear dynamic vibration absorbers, *Journal of Applied Mechanics* 22 (1955) 487–492.
[6] R.S. Haxton, A.D.S. Barr, The autoparametric vibration absorber, *ASME Journal of Engineering for Industry* 94 (1972) 119–125.
[7] A. Vyas, A.K. Bajaj, Dynamics of autoparametric vibration absorbers using multiple pendulums, *Journal of Sound and Vibration* 246 (2001) 115–135.
[8] S. Oueini, C.-M. Chin, A. Nayfeh, Dynamics of a cubic nonlinear vibration absorber, *Nonlinear Dynamics* 230 (1999) 283–295.
[9] O.V. Gendelman, L.I. Manevitch, A.F. Vakakis, R. McCloskey, Energy pumping in nonlinear mechanical oscillators: part i—dynamics of the underlying hamiltonian systems, *Journal of Applied Mechanics* 68 (January) (2001) 34–41.
[10] A.F. Vakakis, O.V. Gendelman, Energy pumping in nonlinear mechanical oscillators: part ii—resonance capture, *Journal of Sound and Vibration* 68 (January) (2001) 42–48.
[11] A. Vakakis, O. Gendelman, L. Bergman, D. McFarland, G. Kerschen, Y. Lee, *Nonlinear Targeted Energy Transfer in Mechanical and Structural Systems*, Springer, Dordrecht, 2009.
[12] O.V. Gendelman, Transition of energy to a nonlinear localized mode in a highly asymmetric system of two oscillators, *Nonlinear Dynamics* 25 (2001) 237–253.
[13] Y.S. Lee, A.F. Vakakis, L.A. Bergman, D.M. McFarland, G. Kerschen, Suppression of aeroelastic instability by means of broadband passive targeted energy transfers, part i: theory, *AIAA Journal* 45 (March) (2007) 693–711.
[14] R. Viguié, G. Kerschen, Nonlinear vibration absorber coupled to a nonlinear primary system: a tuning methodology, *Journal of Sound and Vibration* 326 (2009) 780–793.